

# 1 INFLUENCE OF PRIMARY HOMOGENIZATION STEP ON 2 MICROFLUIDIZED EMULSIONS FORMULATED WITH THYME 3 OIL AND APPYCLEAN 6548

4 Luis A. Trujillo-Cayado<sup>a</sup>, M Carmen Alfaro<sup>a\*</sup>, Jenifer Santos<sup>a</sup>, Nuria Calero<sup>a</sup>, and José  
5 Muñoz<sup>a</sup>

6 <sup>a</sup>Departamento de Ingeniería Química, Facultad de Química, Universidad de Sevilla, C/  
7 P. García González, 1, E41012, Sevilla, Spain.

8 \* Corresponding author. M Carmen Alfaro Rodríguez; Tel.: +34 954 557180; fax: +34  
9 954 556447; *E-mail address*: alfaro@us.es

## 10 ABSTRACT

11 This contribution deals with the development of emulsions formulated using thyme  
12 essential oil and a new biomass-derived surfactant. In addition, this work extends our  
13 knowledge concerning the factors that can influence stability and droplet size  
14 distributions of microfluidized emulsions, such as the geometry of the rotor-stator used  
15 and the homogenization rate in the primary homogenization. Stable thyme oil-in-water  
16 emulsions (30 wt%) containing submicron droplets were formed. Interestingly, laser  
17 diffraction results reveal that mean droplet sizes are mainly controlled by homogenization  
18 rates and polydispersity by the rotor-stator geometry used in the first step of  
19 homogenization. In addition, higher droplet sizes for pre-emulsions seem to be a key  
20 factor in order to reduce both the degree of recoalescence and the size of the droplets  
21 in the second homogenization step. Furthermore, higher droplet sizes in the pre-  
22 emulsion favour higher physical stability of the final emulsions. Finally, this research  
23 highlights the importance of controlling primary homogenization conditions for the  
24 physical stability of microfluidized emulsions that contain natural ingredients.

25 **Keywords:** Droplet size; emulsion; Microfluidizer; physical stability; thyme oil

## 26 1. INTRODUCTION

27 There is a growing interest in the use of essential oils, like thyme oil, due to their  
28 antimicrobial activity and biocompatible properties. These properties make them widely  
29 used in fields such as food, pharmaceutical and cosmetics. In addition, these natural  
30 resources have been recognized as GRAS (Generally Recognized As Safe) by U.S.  
31 Food and Drug Administration [1], which makes them the most promising natural  
32 antimicrobials. Thyme oil, obtained from *Thymus vulgaris L.*, is divided into two different

33 classes: red and white. Red thyme oil is the product of the distillation of dried thyme  
34 leaves while white is obtained from red thyme oil re-distillation [2]. The potential  
35 application of white thyme oil as a food preservative to replace synthetic chemicals,  
36 which are potentially toxic to humans, has been demonstrated [3]. Nevertheless, the  
37 major disadvantage of utilizing essential oils is their high volatility and their tendency to  
38 oxidise. Emulsion-based systems are a very attractive way to increase their stability by  
39 reducing their volatility and conserving their biological characteristics [4]. Oil-in-water  
40 emulsions are systems consisting of oil phase dispersed in aqueous phase, usually in  
41 the form of droplets. These systems are important vehicles for the delivery of  
42 hydrophobic bioactive compounds and have found a wide range of applications in many  
43 industries including food, pharmacy, cosmetics and agrochemistry [5–7].

44 Emulsions need an emulsifier since they are thermodynamically unstable. In recent  
45 years, the use of green surfactants has been attracting attention. Appyclean 6548, a new  
46 surfactant derived from wheat waste (alkyl poly pentoside), fulfils all the requirements to  
47 be considered a green surfactant; namely it is derived from renewable resource and  
48 manufactured by environmentally friendly processes. In fact, this emulsifier possesses  
49 the ECOCERT certification.

50 In order to produce emulsions with specific physicochemical and functional properties,  
51 controlling the droplet size distribution is required. Droplet size distributions are strongly  
52 influenced by the emulsification method and conditions used. Emulsions can be  
53 developed using low-energy and high-energy approaches. However, the latter are more  
54 likely to be used in the food or cosmetic field since their scale-up is easier and the  
55 equipment is more readily available. A multitude of homogenizers, such as rotor-stators,  
56 ultrasounds, colloid mills or high-pressure valve homogenizers, can be used to prepare  
57 these systems. Emulsions can be prepared in two steps: primary and secondary  
58 homogenization. The aim of the primary homogenization is to create droplets of  
59 dispersed phase such that a coarse emulsion is formed. The goal of the second step  
60 (secondary homogenization) is to reduce the size of pre-existing droplets, which usually  
61 involves the use of a different homogenizer. There are several studies concerning the  
62 influence of homogenization rate and the device used on physical stability, rheology and  
63 droplet size distribution for emulsion-based systems [8–13]. One homogenizer used in  
64 the second step that has received a lot of attention recently is the Microfluidizer, due to  
65 several results that suggest its use provides narrower distributions at smaller droplet  
66 sizes [14,15]. Some research has been carried out in order to extend our knowledge  
67 about the influence of the number of cycles and homogenization pressure in  
68 Microfluidizers [9,16,17]. Furthermore, the comparison between using single- or dual-

69 channel microfluidizers and one or two interaction chambers have been reported [18–  
70 20]. The main novelty of this research is the study of the influence of the pre-emulsion  
71 properties on the droplet size distribution and physical stability of the final emulsions. For  
72 this reason, the present work aims to provide an exhaustive study of the influence of the  
73 primary homogenization on microfluidized emulsion properties. On top of that, a further  
74 aim of this research was to obtain stable ecological emulsions of thyme oil formulated  
75 with an emulsifier obtained from wheat. The results of this study could be useful to design  
76 and develop functional oil-in-water emulsions.

## 77 **2. MATERIALS AND METHODS**

### 78 *Materials*

79 30 wt% oil-in-water emulsions with a surfactant (Appyclean 6548) concentration of 3 wt%  
80 were prepared using thyme essential oil as dispersed phase. Thyme oil (*Thymus*  
81 *vulgaris*) was purchased from Sigma Aldrich. The emulsifier (Appyclean 6548) used was  
82 an alkyl poly pentoside provided by Wheatoleo. This non-ionic surfactant is solid and  
83 immiscible in water at room temperature. Deionised water obtained from a water  
84 purification system was used for the preparation of all samples. Sodium azide (0.1 wt%)  
85 was added to the formulation in order to inhibit the growth of microorganisms. All of the  
86 chemicals were used as received.

### 87 *Preparation of oil-in-water emulsions*

88 The surfactant was dispersed into the oil phase. 5.55 g of Appyclean 6548 was added to  
89 55.5 g of Thyme essential oil for emulsion batches of 185 g. Then, the surfactant was  
90 melted and dissolved in the essential oil at 70°C in a laboratory oven according to the  
91 supplier's instructions. The continuous phase was prepared by dissolving 0.185 g of  
92 sodium azide in the corresponding amount of water.

93 Two different rotor-stator devices (Ultraturrax T50 with a S50NG45F dispersion unit and  
94 Silverson L5M equipped with an emulsor mesh screen) were used for the primary  
95 homogenization. Pre-emulsions were produced by adding the oil phase at 20 °C to the  
96 continuous phase (deionised water and sodium azide), also at 20 °C, using a syringe  
97 pump at a constant flow rate of 21.67 mL/min during 180 s, and then were homogenized  
98 for an additional 30 s. The homogenization speed was fixed at 2000, 4000 or 6000 rpm  
99 using Ultraturrax T50 or Silverson L5M, so three batches of six different pre-emulsions  
100 were developed. The initial and final temperatures of the emulsion and the amperage  
101 were measured during the primary emulsification process in order to determine the  
102 power density.

103 The secondary homogenization was performed using a Microfluidizer M110P (interaction  
104 chambers F12Y) at 2500 psi (172 bar) for one pass. These conditions were chosen in  
105 order to highlight the importance and influence of the primary homogenization for the  
106 development of oil-in-water emulsions by microfluidization. The outlet sample tube of the  
107 Microfluidizer was cooled with water at 20 °C. The pH values for the continuous phases  
108 and the final emulsions were 5.94 and 6.42, respectively

#### 109 *Droplet size distributions of emulsions*

110 The droplet size distribution and mean droplet sizes were determined using a Malvern  
111 Mastersizer X. Volumetric mean diameter ( $D_{4,3}$ ) was used to compare the droplet sizes  
112 of different emulsions:

$$113 \quad D_{4,3} = \frac{\sum_{i=1}^N n_i d_i^4}{\sum_{i=1}^N n_i d_i^3} \quad \text{Eq. (1)}$$

114 where  $d_i$  is the droplet diameter,  $N$  is the total number of droplets and  $n_i$  is the number of  
115 droplets having a diameter  $d_i$ . Moreover, span was used to study the distribution width of  
116 droplet sizes:

$$117 \quad \text{span} = \frac{D(v,0.9) - D(v,0.1)}{D(v,0.5)} \quad \text{Eq. (2)}$$

118 where  $D(v,0.9)$ ,  $D(v,0.5)$ ,  $D(v,0.1)$  are diameters at 90%, 50% and 10%, respectively, of  
119 cumulative volume. The absorption and refraction indexes used for the continuous  
120 medium (water) were 0.1 and 1, respectively, whereas the refraction index for the  
121 dispersed phase (thyme oil) was 1.50. Droplet size distributions were obtained using a  
122 polydisperse analysis. The influence of aging time on droplet size distributions was  
123 studied during 20 days after preparation to analyze and quantify coalescence/Ostwald  
124 ripening effects.

#### 125 *Analysis of emulsion physical stability*

126 The physical stability of emulsions whose pre-emulsions were obtained with different  
127 emulsification methods was studied and quantified by means of multiple light scattering  
128 measurements (Turbiscan Lab Expert) at 25 °C. The results are presented in the form of  
129 curves which show intensities of backscattering in reference mode (delta-backscattering,  
130  $\Delta\text{BS}\% = \text{BS}_t\% - \text{BS}_0\%$ ) as a function of time and height. The Turbiscan Stability Index  
131 (TSI) has been used for the comparison and estimation of the emulsion stability. The  
132 value of this parameter was calculated with the special computer program using the  
133 equation:

$$134 \quad \text{TSI} = \sum_i \frac{\sum_h |\text{scan}_i - \text{scan}_{i-1}|}{H} \quad \text{Eq. (3)}$$

135 Where  $scan_i$  is the average backscattering for each time (i) of measurement,  $scan_{i-1}$  is  
136 the average backscattering for the (i-1) time of measurement and H is the number of  
137 scans carried out on the sample.

### 138 *Flow Curves*

139 Flow curves for pre-emulsions and emulsions were obtained by means a controlled-  
140 stress rheometer, CS Haake-MARS (Thermo), and a sandblasted Z20 coaxial cylinder  
141 ( $R_i = 1$  cm,  $R_e/R_i = 1.085$ ) at 24 hours of aging time and they were performed at 25 °C.  
142 A step-wise protocol in the 0.1-20 Pa shear stress range was applied. All samples  
143 showed Newtonian behaviour which was fitted to Newton's law.

144 All measurements were done in duplicate and the values shown are the average of the  
145 two replicates.

## 146 **3. RESULTS AND DISCUSSION**

147 Figure 1 illustrates the power density ( $P_v$ ) as a function of the residence time for five  
148 replicates of the pre-emulsion processed at 2000 rpm using a Silverson L5M rotor-stator  
149 device. A decrease in power density values with homogenization time is clearly  
150 observed. The energy density ( $E_v$ ) or mechanical energy input per unit of dispersing  
151 volume for all pre-emulsions was calculated using the power density values by means of  
152 the following equation [21,22]:

$$153 \quad E_v = \int P_v(t)dt = \int \frac{W(N,t)}{\rho_c(t) + \rho_0(t)} dt \quad \text{Eq. (4)}$$

154 Where  $E_v$  is the energy density or energy consumption,  $P_v$  is the power density, W is the  
155 electrical power consumption,  $M_c$  and  $M_0$  are the masses of the continuous and  
156 dispersed phases respectively and  $\rho_c$  and  $\rho_0$  are the densities of the continuous and  
157 dispersed phases respectively, N is the homogenization rate and t is the homogenization  
158 time. Both densities are time dependent due to the increase in temperature during  
159 emulsification.

160 The values of  $E_v$  for all pre-emulsions are shown in table 1. It should be noted that, as  
161 expected, there is an increment in the energy consumption with homogenization rate for  
162 both rotor-stator devices. Interestingly, energy consumption values obtained for the pre-  
163 emulsions developed using an Ultraturrax T50 are much higher than those obtained for  
164 the samples processed with the Silverson L5M rotor–stator device. This fact is probably  
165 due to the differences between the geometries of both rotor-stator devices [23]. The  
166 resulting droplet size distributions (DSDs) for these pre-emulsions are shown in figure 2.

167 Higher homogenization rates in both rotor stator devices lead to the production of smaller  
168 droplets (Table 1). Pre-emulsions developed at 2000 rpm in both rotor-stator devices  
169 show bimodal DSDs. In contrast, monomodal distributions were observed for emulsions  
170 processed above 2000 rpm in both homogenizers. This fact reveals the importance of  
171 higher homogenization rates/energy input in order to reduce the second peak of the  
172 distribution and obtain a monomodal DSD. It is important to note that the use of different  
173 types of rotor-stator did not significantly affect volumetric diameter at the same  
174 homogenization rate. Although the energy consumption values at the same  
175 homogenization rate are different for Silverson L5M and Ultraturrax T50, similar droplet  
176 mean diameters are detected. This result suggests the higher efficiency of Silverson  
177 L5M. Even so, although the mean droplet sizes are similar, some slight differences in  
178 DSD can be observed between the pre-emulsions with SL5M and UT50 at the same  
179 homogenization rate. Thyme essential oil-in-water emulsions processed in Silverson  
180 L5M tend to possess narrower DSD. In these terms, the existence of little holes in  
181 Silverson L5M favours the existence of jets in the velocity profile contrary to UT50, as  
182 previously reported by Ozcan-Tas et al., 2011[24]. It may be the reason why the  
183 polydispersity of emulsions prepared with Silverson L5M is lower than those developed  
184 using UT50.

185 Figure 3 shows, by way of example, the variation in Backscattering in mode reference  
186 ( $\Delta BS\%$ ) as a function of the height of the measuring cell with aging time for pre-emulsions  
187 developed at 2000 rpm with Silverson L5M. All pre-emulsions follow the same  
188 destabilization trend. A marked decrease in BS in the lower zone of the measuring cell  
189 is observed during the first 24 hours. This reduction extends over the whole measuring  
190 cell with aging time. This fact is a clear indication of a creaming process, such as  
191 commonly occurs in dispersed systems such as emulsions [25,26]. This destabilization  
192 mechanism is favoured by the low viscosity of these pre-emulsions (3.71–5.25 mPa·s)  
193 and the high droplet sizes [27]. In order to improve the stability of these emulsions  
194 formulated with thyme oil and Appyclean 6548, a secondary homogenization was carried  
195 out.

196 The DSD of the final emulsions is shown in Figure 4. All microfluidized emulsions exhibit  
197 two populations of droplets, which is probably due to an excess of energy input  
198 (recoalescence). This fact occurs often in emulsions prepared in high pressure  
199 homogenizers and Microfluidizers [17,28]. In order to analyse the recoalescence for  
200 emulsions studied, the data of the second peak were fitted to a Gaussian model:

201 
$$y = y_0 + Ae^{\frac{-(x-x_c)^2}{2w^2}} \quad \text{Eq. (5)}$$

202 where  $y_0$  is the offset,  $x_c$  the centre of the peak,  $w$  the width of the peak and  $A$  the  
203 amplitude.

204 One factor which should be noted is the low degree of recoalescence observed in  
205 microfluidized emulsions whose pre-emulsions were prepared at the lowest  
206 homogenization rate (2000 rpm). This fact can be deduced from the area of the second  
207 peak (table 2), which is lower for emulsions whose pre-emulsions were prepared at 2000  
208 rpm. In addition, microfluidized emulsions processed in UT50 showed a higher degree  
209 of recoalescence than those obtained using SL5M, evidence of which can be seen in the  
210 larger area or higher median value of the second peak (table 2). These facts support the  
211 aforementioned hypothesis concerning over-processing. Moreover, all results suggest  
212 that for thyme essential oil-in-water emulsions formulated with Appyclean 6548 the  
213 homogenization rate in the primary homogenization and, therefore the droplet size of the  
214 pre-emulsion, is a key factor for final emulsions. It seems that bigger droplets in the first  
215 step of homogenization could favour the break-up of the droplets inside the Microfluidizer  
216 chamber. Accordingly, a lower homogenization rate in pre-emulsion, implying higher  
217 droplet sizes, is recommended in order not only to reduce recoalescence in the  
218 Microfluidizer but also to obtain final emulsions with better properties. This fact is evident,  
219 taking into account the volumetric diameter and span values for final emulsions (figure  
220 5). As can be observed in figure 5, there is a noticeable increase in droplet size and  
221 polydispersity with homogenization rate applied in the primary homogenization. Hence,  
222 although higher droplet size in the first step of homogenization could seem a drawback,  
223 results reveal that the break-up of droplets is favoured and recoalescence is less  
224 probable.

225 To study the physical stability of emulsions, the backscattering profiles were analysed at  
226 different storage times in reference mode allowing a better display of the destabilization  
227 processes. Figure 6A and 6B illustrate the variation of delta-backscattering ( $\Delta BS\%$ )  
228 versus measuring cell height as a function of aging time for emulsion with pre-emulsion  
229 processed using Ultraturrax T50 at 2000 and 6000 rpm. Firstly, it should be noted that  
230 the microfluidized emulsions possess higher physical stability than pre-emulsions (see  
231 figure 3), as expected [29]. Final emulsions showed a marked drop in backscattering (a  
232 peak in  $\Delta BS$  curves) in the lower zone of the measuring cell (0-5 mm), which is typical of  
233 migration of droplets; namely a destabilization mechanism by creaming occurs. All  
234 emulsions studied underwent creaming at similar rates (0.048-0.052 mm/day) and  
235 intensities, as can be observed in figures 6A and 6B. This instability is clearly related to  
236 the low Newtonian viscosity they present (7.78-8.80 mPa-s) [27]. Additionally, there is  
237 also a decrease in the BS intensity in the middle zone of the tube, indicative of an

238 increment in mean droplet sizes [6,26]. The decrease in BS intensity in the middle zone  
239 is more marked for the emulsion processed at 6000 rpm (see figure 6B). This behaviour  
240 may be related to flocculation, coalescence or Ostwald ripening. In order to discern  
241 between these destabilization processes as well as quantify the destabilization  
242 mechanism that provokes this variation, the evolution over time of droplet size  
243 distributions, droplet mean diameters and span was analysed.

244 Figure 7 shows the droplet size distributions with aging time for the microfluidized  
245 emulsion whose pre-emulsion was developed using Ultraturrax T50 at 2000 and 6000  
246 rpm. This figure illustrates a shift of DSD towards higher droplet sizes and a reduction in  
247 polydispersity for both emulsions. It is more clearly observed for 6000 rpm emulsion,  
248 which is totally consistent with the results obtained from laser diffraction measurements.  
249 This behaviour suggests that the increase in mean diameters observed with the multiple  
250 light scattering technique is due to a destabilization mechanism by Ostwald ripening [30].  
251 This result is consistent with works reported by other authors and it is typically observed  
252 in essential oil-in-water emulsions [31,32]. All emulsions presented an increase in  
253 volumetric mean diameter and a reduction in span, which is shown in figure 8. The  
254 variations of Volumetric diameter and span values from day 20 to day 1 were calculated  
255 as follows:

$$256 \quad \Delta D_{4,3} = \frac{D_{4,3 \text{ day } 20} - D_{4,3 \text{ day } 1}}{D_{4,3 \text{ day } 1}} \quad \text{Eq. (6)}$$

257

$$258 \quad \Delta span = \frac{span_{\text{day } 20} - span_{\text{day } 1}}{span_{\text{day } 1}} \quad \text{Eq. (7)}$$

259 A clear influence of both the primary homogenization rate and the rotor-stator device  
260 used for the development of the pre-emulsions on the evolution of both the volumetric  
261 mean diameter and span of microfluidized emulsions can be observed. In this sense,  
262 emulsions developed at higher homogenization rates presented the major variations in  
263 both parameters and emulsions processed with SL5M showed smaller variations in  
264 droplet sizes and span than their counterparts processed using UT50. These facts are  
265 related to the higher polydispersity these emulsions exhibited at 24 hours (see figure 4),  
266 i.e. more polydispersity favours destabilization by Ostwald ripening [33].

267 Turbiscan Stability Index (TSI) values as a function of aging time for all thyme oil  
268 microfluidized emulsions are shown in figure 9. This parameter, obtained in the 0-30 mm  
269 zone, allows global physical stability (considering all destabilization mechanisms) to be  
270 analysed for these dispersed systems. High values of TSI involve poor physical stability.  
271 In this way, the influence of the homogenization rate used in the primary homogenization



272 on the final emulsion physical stability is demonstrated. Two trends can be clearly  
273 observed, as expected. On the one hand, the use of a lower homogenization rate during  
274 the primary homogenization allowed lower TSI values to be obtained. On the other hand,  
275 microfluidized emulsion whose pre-emulsion was prepared in Silverson L5M showed  
276 better physical stability than those whose pre-emulsion was developed using Ultraturrax  
277 T50. These facts are related to the aforementioned differences in polydispersity, i.e.  
278 higher polydispersity involves higher TSI values. Hence, the microfluidized emulsion  
279 whose primary homogenization was in Silverson L5M at the lowest homogenization rate  
280 presented the best global physical stability and the lowest droplet size and polydispersity.  
281 This fact demonstrates the necessity for a pre-emulsion with a relatively large droplet  
282 size in order to allow the Microfluidizer to play its role in forming finer emulsions.

## 283 **CONCLUSIONS**

284 Stable and concentrated thyme oil-in-water emulsions formulated with a biomass-  
285 derived surfactant obtained from renewable resources have been developed. No  
286 significant differences in droplet sizes for pre-emulsions prepared using Silverson L5M  
287 or Ultraturrax T50 at the same homogenization rate were observed. However, the energy  
288 consumption for Ultraturrax T50 was much higher than that of Silverson L5M, suggesting  
289 the greater efficiency of the latter. Results obtained for these pre-emulsions indicate that  
290 mean droplet sizes are mainly controlled by homogenization rates and polydispersity by  
291 rotor-stator geometry. All pre-emulsions showed low physical stability involving a  
292 creaming destabilization process due to their high mean droplet sizes, high polydispersity  
293 and low viscosity.

294 Microfluidized emulsions showed submicron mean droplet sizes but a recoalescence  
295 process was observed. This effect was favoured by higher homogenization rates and the  
296 use of Ultraturrax T50 in the primary homogenization. Therefore, the droplet size  
297 distribution of the pre-emulsions is a key factor that strongly influences the droplet size  
298 distribution of the final emulsions. Higher mean droplet sizes for pre-emulsions could  
299 favour the break-up of the droplets inside the high-pressure homogenizer chamber,  
300 allowing lower droplet size in microfluidized emulsions to be obtained. Hence, the coarse  
301 emulsion developed using Silverson L5M at 2000 rpm produced the microfluidized  
302 emulsion with the narrowest droplet size distribution and the lowest mean droplet sizes.  
303 All microfluidized emulsions presented higher physical stability than those developed  
304 only with a rotor-stator device. However, a creaming process and an increase in droplet  
305 size were observed in final emulsions. These variations in droplet sizes involved a  
306 reduction in span with aging time, which suggests destabilization by Ostwald ripening.

307 This phenomenon was more marked for those microfluidized emulsions whose pre-  
308 emulsions were developed at higher homogenization rates.

309 This work demonstrates that a tight control of the primary homogenization conditions in  
310 the development of microfluidized emulsions is required. Results obtained from this work  
311 can be useful for further design and fabrication of functional emulsions suitable for  
312 utilization within the food, chemical, pharmaceutical, personal care, and other industries.

### 313 **ACKNOWLEDGMENTS**

314 The financial support received (Project CTQ2015-70700-P) from the Spanish Ministerio  
315 de Economía y Competitividad and from the European Commission (FEDER  
316 Programme) is kindly acknowledged.

317

### 318 **References**

- 319 [1] USA, Code of Federal Regulations, Title 21 Food and drugs, Chapter I Food and  
320 Drug Administration Department of Health and Human Services, Subchapter B–  
321 Food for Human Consumption, Part 182–Substances Generally Recognized as  
322 Safe. Sec. 182.20 Essential oils (2011).
- 323 [2] I.M. Martins, S. N. Rodrigues, F. Barreiro, A. E. Rodrigues, J. Microencapsul.  
324 26(8) (2012) 667-675.
- 325 [3] A.A. Dobre, V. Gagiú, N. Petru, Rom. Biotechnol. Lett. 16(6) (2011) 119–25.
- 326 [4] S. Rodríguez-Rojo, S. Varona, M. Núñez,, M.J. Cocero, Ind. Crops Prod. 37(1)  
327 (2012) 137–40.
- 328 [5] K.C. Powell, R. Damitz, A. Chauhan, Int. J. Pharm. 521(1) (2017) 8–18.
- 329 [6] L.A. Trujillo-Cayado, M.C. Alfaro, J. Muñoz, Colloids Surfaces A Physicochem.  
330 Eng. Asp. 536 (2018) 198–203.
- 331 [7] M. Matos, A. Laca, F. Rea, O. Iglesias, M. Rayner, G. Gutiérrez, J. Food Eng.  
332 222 (2018) 207–17.
- 333 [8] S. Aben, C. Holtze, T. Tadros, P. Schurtenberger, Langmuir 28(21) (2012)  
334 7967–75.
- 335 [9] J. Santos, L.A. Trujillo-Cayado, N. Calero, M.C. Alfaro, J. Muñoz, J. Ind. Eng.  
336 Chem. (2016).
- 337 [10] S.M. Jafari, Y. He, B. Bhandari, Eur. Food Res. Technol. 225(5–6) (2007) 733–  
338 41.
- 339 [11] J. Santos, N. Calero, J. Munoz, RSC Adv. 62(6) (2016) 57563–8.
- 340 [12] S. Mahdi Jafari,, Y. He,, B. Bhandari, Int. J. Food Prop. 9(3) (2006) 475–85.
- 341 [13] U. El-Jaby, M. Cunningham, T.F.L. McKenna, Ind. Eng. Chem. Res. 48(22)  
342 (2009) 10147–51.

343 [14] J.M. Perrier-Cornet, P. Marie, P. Gervais, J. Food Eng. 66(2) (2005) 211–7.  
344 [15] K.B. Strawbridge, E. Ray, F.R. Hallett, S.M. Tosh, D.G. Dalgleish, J. Colloid  
345 Interface Sci. 171(2) (1995) 392–8.  
346 [16] S.S. Galooyak, B. Dabir, J. Food Sci. Technol. 52(5) (2015) 2558–71.  
347 [17] L.A. Trujillo-Cayado, J. Santos, M.C. Alfaro, N. Calero, J. Muñoz, Ind. Eng.  
348 Chem. Res. 55(27) (2016) 7259–66.  
349 [18] L.A. Trujillo-Cayado, J. Santos, P. Ramírez, M.C. Alfaro, J. Muñoz, J. Clean.  
350 Prod. 178 (2018) 723–30.  
351 [19] L. Bai, D.J. McClements, J. Colloid Interface Sci. 466 (2016) 206–12.  
352 [20] L. Bai, S. Huan, J. Gu, D.J. McClements, Food Hydrocoll. 61 (2016) 703–11.  
353 [21] H. Schubert, K. Ax, O. Behrend, Trends Food Sci. Technol. 14(1–2) (2003) 9–  
354 16.  
355 [22] P. Walstra, P.E.A. Smulders, Mod. Asp. Emuls. Sci. (1998) 56–99.  
356 [23] H. Schubert, R. Engel, Chem. Eng. Res. Des. 82(9) (2004) 1137–43.  
357 [24] G. Özcan-Taşkin, D. Kubicki, G. Padron, Can. J. Chem. Eng. 89(5) (2011)  
358 1005–17. 10.1002/cjce.20553.  
359 [25] J. Santos, N. Calero, J. Muñoz, Chem. Eng. Res. Des. 100 (2015) 261–7.  
360 [26] O. Mengual, G. Meunier, I. Cayré, K. Puech, P. Snabre, Talanta 50(2) (1999)  
361 445–56.  
362 [27] D.J. McClements, Crit. Rev. Food Sci. Nutr. 47(7) (2007) 611–49.  
363 [28] S.M. Jafari, E. Assadpoor, Y. He., B. Bhandari, Food Hydrocoll. 22(7) (2008)  
364 1191–202. 10.1016/j.foodhyd.2007.09.006.  
365 [29] D.J. McClements, Food emulsions: principles, practices, and techniques, CRC  
366 press, 2015.  
367 [30] E. Nazarzadeh, T. Anthonypillai, S. Sajjadi, J. Colloid Interface Sci. 397 (2013)  
368 154–62.  
369 [31] Y. Chang, L. McLandsborough, D.J. McClements, Food Chem. 172 (2015) 298–  
370 304.  
371 [32] V. Ryu, D.J. McClements, M.G. Corradini, L. McLandsborough, Food Chem.  
372 245(September 2017) (2018) 104–11. 10.1016/j.foodchem.2017.10.084.  
373 [33] T.J. Wooster, M. Golding, P. Sanguansri, Langmuir 24(22) (2008) 12758–65.  
374  
375  
376  
377  
378  
379

380 **Tables**

381

382 Table 1.- Energy consumption ( $E_v$ ) and volumetric mean diameter ( $D_{4,3}$ ) as a function of  
 383 homogenization rate for all emulsions processed using only a rotor-stator device

384

Rotor-stator device	Homogenization rate (rpm)	$E_v$ ( $\text{kJ}\cdot\text{m}^{-3}$ )	$D_{4,3}$ ( $\mu\text{m}$ )
UltraTurrax T50 (UT50)	2000	349.50 $\pm$ 2.89	6.36 $\pm$ 0.44
	4000	382.02 $\pm$ 8.87	2.56 $\pm$ 0.15
	6000	442.77 $\pm$ 2.74	2.02 $\pm$ 0.11
Silverson L5M (SL5M)	2000	126.31 $\pm$ 2.22	7.01 $\pm$ 0.52
	4000	141.14 $\pm$ 3.21	2.58 $\pm$ 0.13
	6000	163.67 $\pm$ 4.58	1.84 $\pm$ 0.10

393

394 Table 2. Centre and area of the second peaks of the DSD for microfluidized emulsions.  
 395 Parameters obtained from Gaussian model.

396

Rotor-stator device	Homogenization rate (rpm)	$X_c$ ( $\mu\text{m}$ )	Peak Area ( $\%\cdot\mu\text{m}$ )
UltraTurrax T50 (UT50)	2000	3.57	5.06
	4000	2.85	10.91
	6000	2.94	12.30
Silverson L5M (SL5M)	2000	2.05	1.57
	4000	2.12	10.56
	6000	2.30	13.24

403

404

405

406

407

408

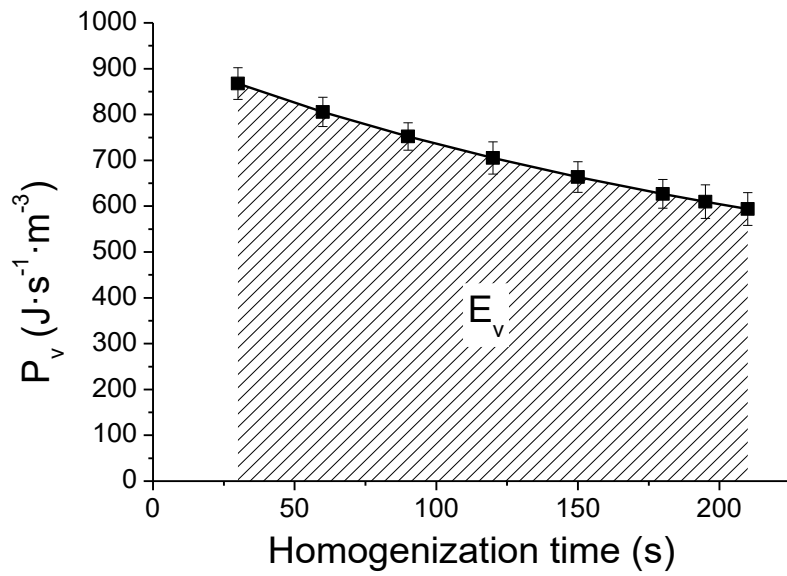
409

410

411

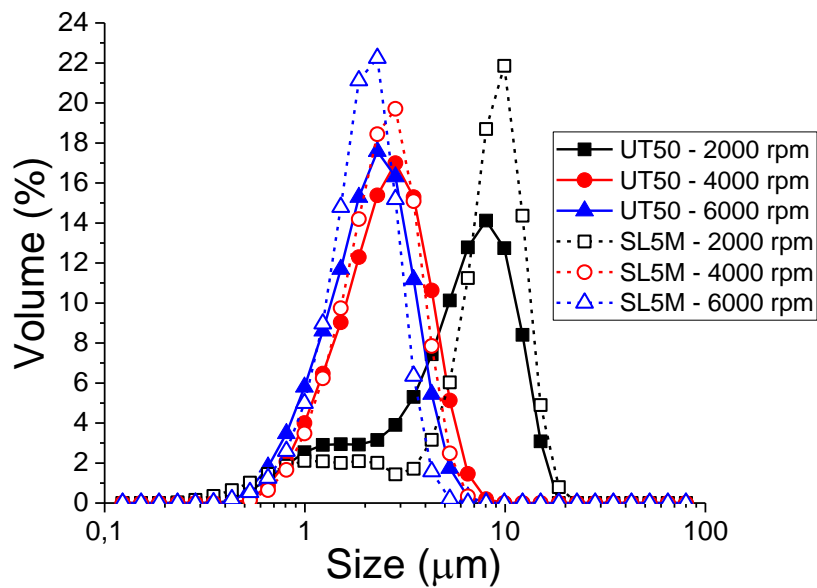
412

413 **Figure and figure captions**



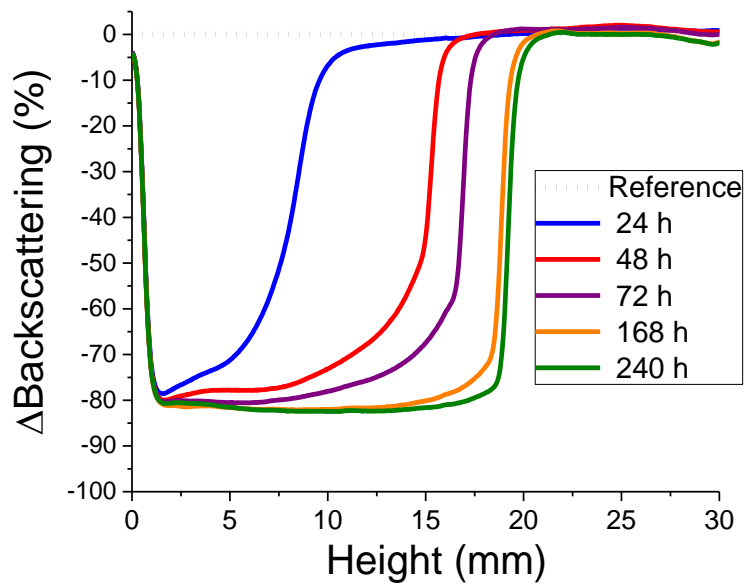
414

415 Figure 1.- Power density ( $P_v$ ) for five replicates of the emulsions processed using a  
416 Silverson L5M at 2000 rpm as a function of homogenization time. Vertical bars indicate  
417 standard deviation data



418

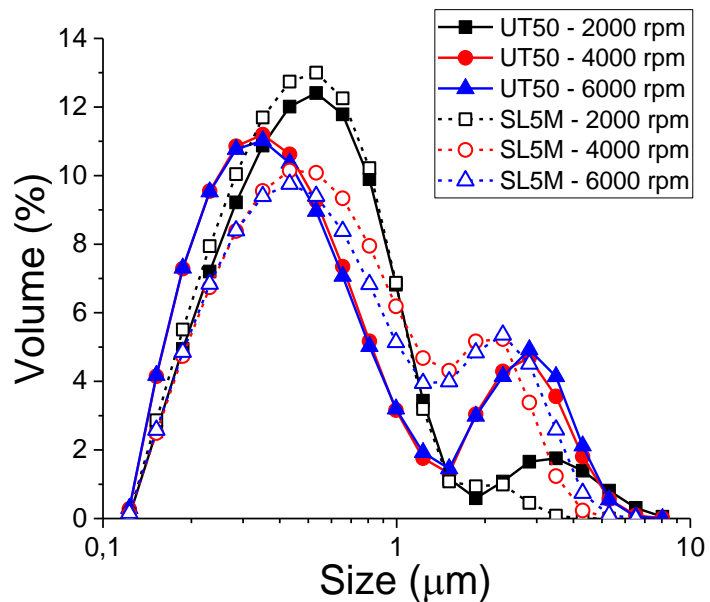
419 Figure 2. Droplet size distributions for pre-emulsions aged for 24 hours as a function of  
420 homogenization rate and rotor-stator device.



421

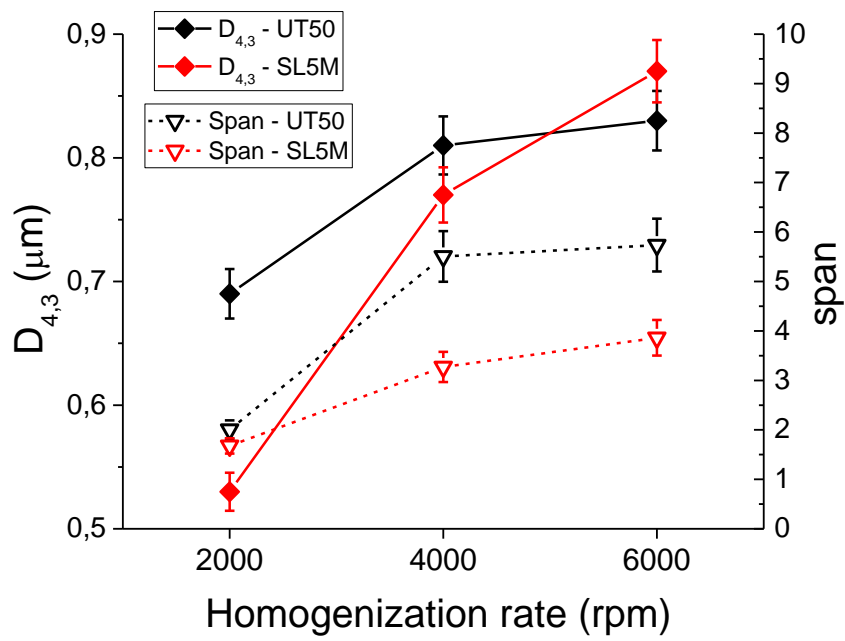
422 Figure 3. Backscattering versus container height as a function of aging time in reference  
 423 mode for the pre-emulsion processed with Silverson L5M at 2000 rpm. Temperature: 25  
 424 °C

425



426

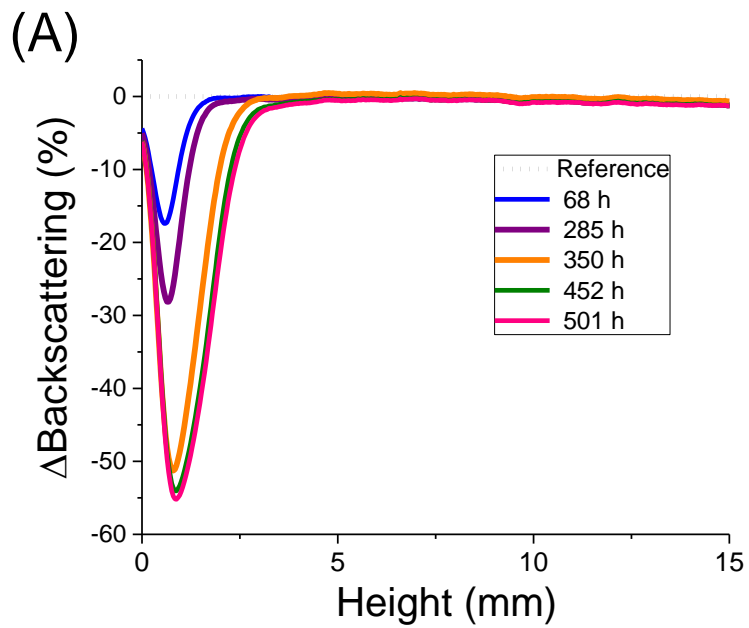
427 Figure 4. Droplet size distributions for final emulsions aged for 24 hours as a function of  
 428 homogenization rate and rotor-stator device used for the development of the pre-  
 429 emulsion.



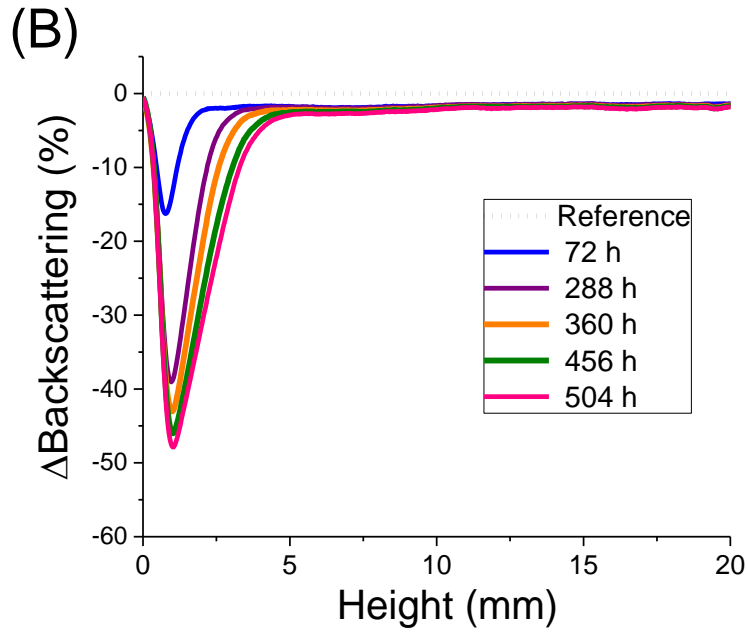
430

431 Figure 5. Volumetric mean diameters and span values as a function of homogenization  
 432 rate for final emulsions aged for 24 hours.

433

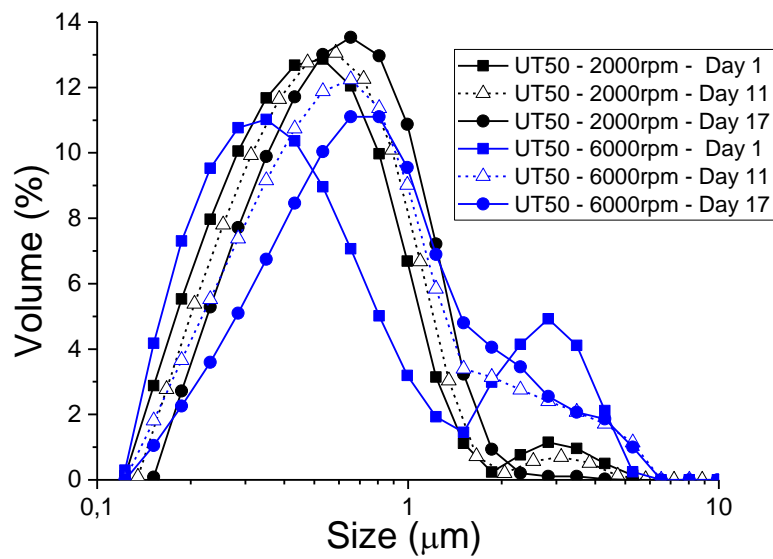


434



435

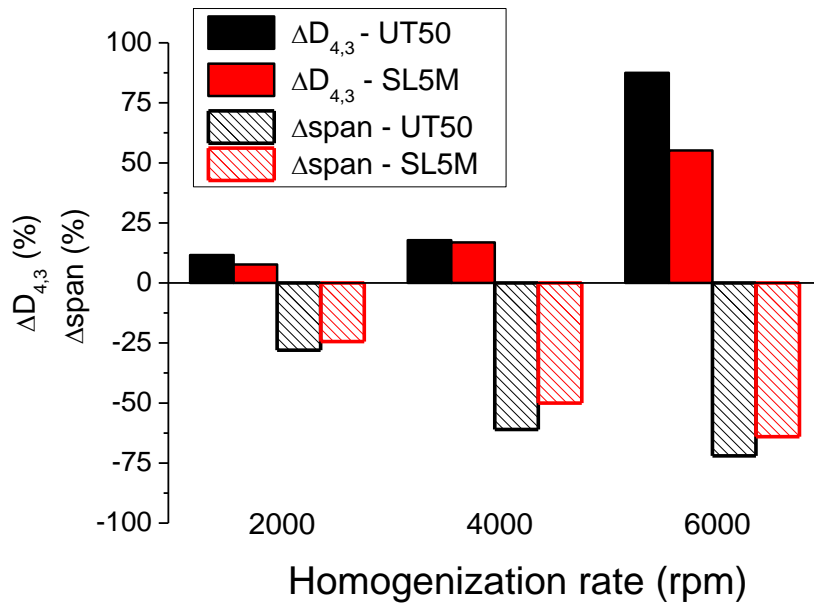
436 Figure 6. Backscattering versus container height as a function of aging time in reference  
 437 mode for final emulsions whose pre-emulsion was obtained with Ultraturrax T50 at (A)  
 438 2000 rpm and (B) 6000 rpm. Temperature: 25 °C



439

440 Figure 7. Droplet size distributions as a function of aging time for final emulsions whose  
 441 pre-emulsion was developed using Ultraturrax T50 at 2000 rpm and 6000 rpm.



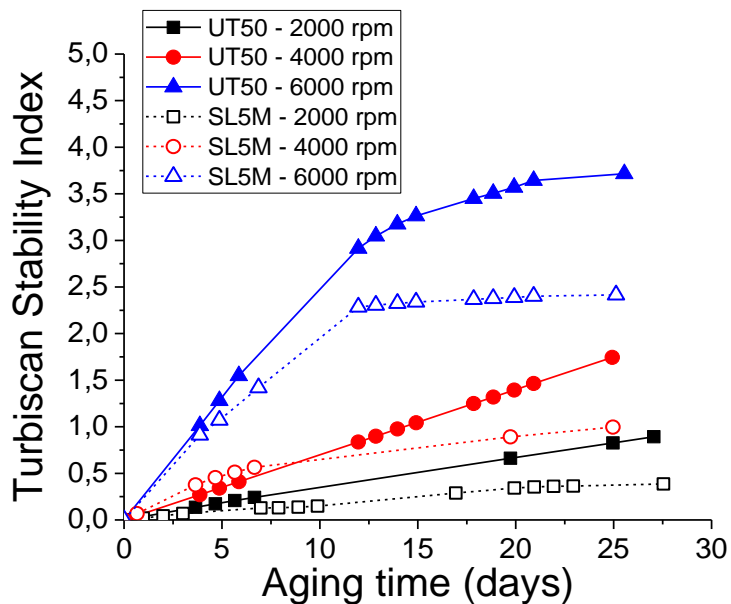


442

443 Figure 8. Variation of volumetric mean diameters and span values for final emulsions  
 444 between day 1 and day 20 as a function of the homogenization rate applied in the primary  
 445 homogenization.

446

447



448

449 Figure 9. Turbiscan Stability Index of microfluidized emulsions as a function of aging  
 450 time.

451